



Vibration Analysis of Laminated Composite Plate under Thermo-Mechanical Loading

Prof. Dr. Adnan Naji Jameel
University of Baghdad
College of Engineering
Mechanical Engineering Dep
adnanaji2004@yahoo.com

Eng. Rasha Mohammed Hussien
University of Baghdad
College of Engineering
Mechanical Engineering Dep.
mechanicalflower99@yahoo.com

ABSTRACT

The present study focused mainly on the vibration analysis of composite laminated plates subjected to thermal and mechanical loads or without any load (free vibration). Natural frequency and dynamic response are analyzed by analytical, numerical and experimental analysis (by using impact hammer) for different cases. The experimental investigation is to manufacture the laminates and to find mechanical and thermal properties of glass-polyester such as longitudinal, transverse young modulus, shear modulus, longitudinal and transverse thermal expansion and thermal conductivity. The vibration test carried to find the three natural frequencies of plate. The design parameters of the laminates such as aspect ratio, thickness ratio, boundary conditions and lamination angle were investigated using classical laminated plate theory (CLPT) and Finite element coded by ANSYS, in addition to the design parameters of dynamic response such as load type with respect to time, x and y dimension and temperature value for simply supported symmetric cross ply. The main conclusion was the natural frequency could increase and decrease depending on the boundary conditions, thickness ratio, and lamination angle, the aspect ratio of the plate. Present of temperature could increase dynamic response of plate also depending on lamination angle, type of mechanical load and the value of temperature.

Keywords: composite laminated plate, natural frequency, dynamic response, classical laminated plate theory, ANSYS, thermo-mechanical load.

تحليل الاهتزازات للصفائح المركبة تحت تأثير احمال ميكانيكية حرارية

مهندسة رشا محمد حسين

أ.د. عدنان ناجي جميل

الخلاصة:

هذه الدراسة ركزت بشكل رئيسي على تحليل الاهتزاز للصفائح المركبة معرضة للأحمال الحرارية و الميكانيكية أو دون أي تحميل (الاهتزاز الحر). ويتم تحليل الترددات الطبيعية والاستجابة الديناميكية عن طريق التحليل النظري، التحليل العددي والعملي (باستخدام المطرقة) لمختلف الحالات. في الجانب العملي تم تصنيع الصفائح المركبة المصنوعة من الالياف الزجاجية والبوليستر لإيجاد الخواص الحرارية والميكانيكية مثل معامل يونك الطولي والعرضي و معامل القص والتمدد الحراري الطولي والعرضي و التوصيل الحراري. تم عمل اختبار الاهتزاز للعثور على الترددات الطبيعية الثلاثة للصفحة. كما تم بحث عناصر تصميم شرائح مثل نسبة العرض إلى الارتفاع، ونسبة سماكة وشروط الحدود وزاوية التصفيح باستخدام النظرية الكلاسيكية CLPT و طريقة العناصر المحددة المبرمجة باستخدام برنامج

ANSYS. بالإضافة إلى عناصر تصميم الاستجابة الديناميكية مثل نوع الحمولة المتغيرة مع الزمن، أو احداثيات x و y وقيمة درجة الحرارة للصفائح المركبة المثبتة التثبيت البسيط simply supported المتماثلة. وكان الاستنتاج الرئيسي ان التردد الطبيعي يمكن ان يقل او يزيد تبعا لشروط الحدود، ونسبة سماكة، وزاوية التصفيح، ونسبة العرض إلى الارتفاع للصفحة . وزيادة الاستجابة الديناميكية للصفحة اعتمادا أيضا على زاوية التصفيح، ونوع الحمولة الميكانيكية وقيمة درجة الحرارة.

الكلمات الرئيسية: صفائح مركبة، الاهتزاز الطبيعي، الاستجابة الديناميكية، النظرية الكلاسيكية للصفائح الطباقية، حمل حراري ميكانيكي.

1. INTRODUCTION

1.1 General

During the last decades, needs for *composite materials* which contain two or more types of materials mixed together homogenously have appeared.

Composite materials have many advantages such as high strength with low weight compared with traditional engineering materials; furthermore, their properties can be controlled during mixing of their components to meet the suitable design requirements. Ref.[Reddy J.N.] Study of vibration of thin plates is an extremely important area owing to its wide variety use of engineering applications. It is essential for a design engineer to have a prior knowledge of the first few modes of vibration characteristics before finalizing the design of a given structure. Many researches had studied free vibration analysis and vibration of plate under mechanical or thermal or thermo-mechanical loading.

Dobyns, A.L., 1981, analysed simply supported orthotropic plates subjected to static and dynamic loading conditions presented the first shear deformation theory. Transient loading conditions considered included sine, rectangular, and triangular pulses. **Reddy, J. N., 1982**, presented two different lamination schemes, under appropriate boundary conditions and sinusoidal distribution of the transverse load. The exact solution was obtained by integrated numerically using Newmark's direct integration method. **Chorng-Fuh Liu and Chih-Hsing Huang, 1996** performed a vibration analysis of laminated composite plates subjected to temperature change. The first order shear deformation theory of a plate is employed. The resulting finite element formulation leads to general nonlinear and coupled simulation

equations and calculate the frequencies of vibration of a symmetric cross-ply plate. **Hui-Shen Shen, et.al, 2003**, studied the dynamic response of shear deformable laminated plates exposed to thermo-mechanical loading and resting on a two-parameter elastic foundation. The formulation is based on higher order shear deformable plate theory and includes the plate foundation interaction and thermal effects due to temperature rise. Effects of foundation stiffness, plate side-to-thickness ratio, and temperature rise on the dynamic response are studied.

Metin Aydogdu and Taner Timarci, 2007, presented numerical results for vibration frequencies of anti-symmetric angle-ply laminated thin square composite plates having different boundary conditions. The Ritz method, along with the displacement assumed in the form of simple polynomials, is applied to solve the problems. **Kullasup P. et al., 2010**, analysed Free vibration of symmetrically laminated composite rectangular plates with various boundary conditions by an extended Kantorovich method, in which a separable function to the dynamic-system energy equation is applied in order to reduce the partial differential equations to ordinary differential equations in the direction of x , y coordinates with a constant coefficient. The beam function is used as an initial trial function in the iterative calculation, which is employed to evaluate the natural frequency and force the final solution needed to satisfy the boundary conditions. **Suresh K. J. et al., 2011**, developed an analytical procedure is to investigate the free vibration characteristics of different laminated composite plates based on higher order shear



displacement model with zig-zag function. This function improves slope discontinuities at the interfaces of laminated composite plates. The related functions are obtained using the dynamic version of principle of virtual work or Hamilton’s principle. The solutions are obtained using Navier’s method.

The point of originality of the present work is how to derive the analytical solution of free vibration for composite laminated plates by classical laminated plate theory for the first time, by applied different type of boundary condition on the symmetric cross-ply composite laminated plates using levy solution. Then derived the equation of motion for transient vibration (with or without the temperature effect) and solving it by Newmark direct integration method. Thermal and mechanical properties, natural frequency for composite plate made from (glass-polyester) with fiber volume fraction (0.3) are determined experimentally.

Also Finite element coded by ANSYS14used in this thesis to find natural frequency and transient response of composite laminate plate.

2. ANALYTICAL SOLUTION (CLASSICAL LAMINATE PLATE THEORY)

2.1 Natural Frequency

2.1.1 Displacement

Classical lamination theory (CLPT) based on the Kirchhoff hypothesis based on assuming the straight line perpendicular to the mid surface before deformation remains straight after deformation which means neglecting shear strains and transverse normal strain and stress in the analysis of laminated composite plates. Ref.[Reddy J.N.]

$$u(x, y, t) = u_o(x, y, t) - z \frac{\partial w_o}{\partial x} \tag{1. a}$$

$$v(x, y, t) = v_o(x, y, t) - z \frac{\partial w_o}{\partial y} \tag{1. b}$$

$$w(x, y, t) = w_o(x, y) \tag{1. c}$$

Where $\frac{\partial w_o}{\partial x}$, $\frac{\partial w_o}{\partial y}$ denote the rotations about y and x axis respectively.

u_o, v_o and w_o denote the displacement components along (x, y, z) directions respectively of a point on the mid-plane (i.e....z=0).

2.1.2 Stress and strain

The total strains can be written as follows

$$\begin{Bmatrix} \epsilon_{xx} \\ \epsilon_{yy} \\ \gamma_{xy} \end{Bmatrix} = \begin{Bmatrix} \epsilon_{xx}^{(0)} \\ \epsilon_{yy}^{(0)} \\ \gamma_{xy}^{(0)} \end{Bmatrix} + z * \begin{Bmatrix} \epsilon_{xx}^{(1)} \\ \epsilon_{yy}^{(1)} \\ \gamma_{xy}^{(1)} \end{Bmatrix} = \begin{Bmatrix} \frac{\partial u_o}{\partial x} \\ \frac{\partial v_o}{\partial y} \\ \frac{\partial u_o}{\partial y} + \frac{\partial v_o}{\partial x} \end{Bmatrix} + z * \begin{Bmatrix} -\frac{\partial^2 w_o}{\partial x^2} \\ -\frac{\partial^2 w_o}{\partial y^2} \\ -2 * \frac{\partial^2 w_o}{\partial x \partial y} \end{Bmatrix} \tag{2}$$

Where $(\epsilon_{xx}^{(0)}, \epsilon_{yy}^{(0)}, \gamma_{xy}^{(0)})$ are the membrane strains and $(\epsilon_{xx}^{(1)}, \epsilon_{yy}^{(1)}, \gamma_{xy}^{(1)})$ are the flexural (bending) strains, known as the curvatures [Reddy J.N.]. The transformed stress-strain relations of an orthotropic lamina in a plane state of stress are; for \bar{Q}_{ij} see [Reddy J.N.]

$$\begin{Bmatrix} \sigma_{xx} \\ \sigma_{yy} \\ \sigma_{xy} \end{Bmatrix}_k = \begin{bmatrix} \bar{Q}_{11} & \bar{Q}_{12} & \bar{Q}_{16} \\ \bar{Q}_{12} & \bar{Q}_{22} & \bar{Q}_{26} \\ \bar{Q}_{16} & \bar{Q}_{26} & \bar{Q}_{66} \end{bmatrix}_k \begin{Bmatrix} \epsilon_{xx} \\ \epsilon_{yy} \\ \gamma_{xy} \end{Bmatrix} \tag{3}$$

The resultant of inplane force N_{xx}, N_{yy} and N_{xy} and moments M_{xx}, M_{yy} and M_{xy} acting on a laminate are obtained by integration of the stress in each layer or lamina through the laminate thickness. Knowing the stress in terms of the displacement, we can obtain the inplane force resultants $N_{xx}, N_{yy}, N_{xy}, M_{xx}, M_{yy}$ and M_{xy} .

The inplane force resultants are defined as

$$\begin{Bmatrix} N_{xx} \\ N_{yy} \\ N_{xy} \end{Bmatrix} = \sum_{k=1}^N \int_{z_k}^{z_{k+1}} \begin{Bmatrix} \sigma_{xx} \\ \sigma_{yy} \\ \sigma_{xy} \end{Bmatrix}_k dz \tag{4.a}$$

Where σ_x, σ_y and σ_{xy} are normal and shear stress.

$$\begin{Bmatrix} N_{xx} \\ N_{yy} \\ N_{xy} \end{Bmatrix} = \begin{bmatrix} A_{11} & A_{12} & A_{16} \\ A_{12} & A_{22} & A_{26} \\ A_{16} & A_{26} & A_{66} \end{bmatrix} \begin{Bmatrix} \varepsilon_{xx}^0 \\ \varepsilon_{yy}^0 \\ \gamma_{xy}^0 \end{Bmatrix} + \begin{bmatrix} B_{11} & B_{12} & B_{16} \\ B_{12} & B_{22} & B_{26} \\ B_{16} & B_{26} & B_{66} \end{bmatrix} \begin{Bmatrix} \varepsilon_{xx}^1 \\ \varepsilon_{yy}^1 \\ \gamma_{xy}^1 \end{Bmatrix} \quad (4.b)$$

$$\begin{Bmatrix} M_{xx} \\ M_{yy} \\ M_{xy} \end{Bmatrix} = \sum_{k=1}^N \int_{z_k}^{z_{k+1}} \begin{Bmatrix} \sigma_{xx} \\ \sigma_{yy} \\ \sigma_{xy} \end{Bmatrix}_k z \, dz \quad (5.a)$$

$$\begin{Bmatrix} M_{xx} \\ M_{yy} \\ M_{xy} \end{Bmatrix} = \begin{bmatrix} B_{11} & B_{12} & B_{16} \\ B_{12} & B_{22} & B_{26} \\ B_{16} & B_{26} & B_{66} \end{bmatrix} \begin{Bmatrix} \varepsilon_{xx}^0 \\ \varepsilon_{yy}^0 \\ \gamma_{xy}^0 \end{Bmatrix} + \begin{bmatrix} D_{11} & D_{12} & D_{16} \\ D_{12} & D_{22} & D_{26} \\ D_{16} & D_{26} & D_{66} \end{bmatrix} \begin{Bmatrix} \varepsilon_{xx}^1 \\ \varepsilon_{yy}^1 \\ \gamma_{xy}^1 \end{Bmatrix} \quad (5.b)$$

Here, A_{ij} are the extensional stiffness, B_{ij} the coupling stiffness, and D_{ij} the bending stiffness.

$$A_{ij} = \sum_{k=1}^N (\bar{Q}_{ij})_k (z_{k+1} - z_k) \quad (6.a)$$

$$B_{ij} = \frac{1}{2} \sum_{k=1}^N (\bar{Q}_{ij})_k (z_{k+1}^2 - z_k^2) \quad (6.b)$$

$$D_{ij} = \frac{1}{3} \sum_{k=1}^N (\bar{Q}_{ij})_k (z_{k+1}^3 - z_k^3) \quad (6.c)$$

2.1.3 Equation of motion

The equations of motion are obtained by setting the coefficient of δu_0 , δv_0 , δw_0 to zero separately

$$\frac{\partial N_{xx}}{\partial x} + \frac{\partial N_{xy}}{\partial y} = I_0 \frac{\partial^2 u}{\partial t^2} - I_1 \frac{\partial^2 w}{\partial x \partial t^2} \quad (7.a)$$

$$\frac{\partial N_{xy}}{\partial x} + \frac{\partial N_{yy}}{\partial y} = I_0 \frac{\partial^2 v}{\partial t^2} - I_1 \frac{\partial^2 w}{\partial y \partial t^2} \quad (7.b)$$

$$\begin{aligned} & \frac{\partial^2 M_{xx}}{\partial x^2} + 2 \frac{\partial^2 M_{xy}}{\partial x \partial y} + \frac{\partial^2 M_{yy}}{\partial y^2} + \bar{N}_{xx} \frac{\partial^2 w}{\partial x^2} + \bar{N}_{yy} \frac{\partial^2 w}{\partial y^2} + \\ & \bar{N}_{xy} \frac{\partial^2 w}{\partial x \partial y} = I_0 \frac{\partial^2 w}{\partial t^2} + I_1 \left(\frac{\partial^3 u}{\partial x \partial t^2} + \frac{\partial^3 v}{\partial y \partial t^2} \right) - \\ & I_2 \left(\frac{\partial^4 w}{\partial x^2 \partial t^2} + \frac{\partial^4 w}{\partial y^2 \partial t^2} \right) - q(x, y, t) \end{aligned} \quad (7.c)$$

Where

$$(I_0, I_1, I_2) = \sum_{k=1}^N \int_{z_{k-1}}^{z_k} \rho^{(k)}(1, z, z^2) dz \quad (8)$$

$\rho^{(k)}$ being the material density of k^{th} layer and $q(x,y,t)$ is a dynamic force subjected on a system. For natural frequency $q(x,y,t)$ and $\bar{N}_{xx}, \bar{N}_{yy}$ and \bar{N}_{xy} equal to zero.

These equations of motion (7 a-c) can be expressed in terms of displacements (δu_0 , δv_0 , δw_0) by substituting the forces results from Eqs. (4 ,5,8) into Eq. (7.a) to(7.c) and get partial differential equations, then the analytical solution done by levy method as derived in [Reddy J.N.].

2.2 Dynamic Response

2.2.1 Equation of motion

In classical laminate plate theory, the equations of motion derived using the dynamic version of the principle of virtual displacements. The derivation and all equation for no temperature effect discussed in section (2.1). but the stress strain relations when there were temperature change is [9]

$$\begin{Bmatrix} \varepsilon_{xx} \\ \varepsilon_{yy} \\ \gamma_{xy} \end{Bmatrix} = \begin{Bmatrix} \varepsilon_{xx}^{(0)} \\ \varepsilon_{yy}^{(0)} \\ \gamma_{xy}^{(0)} \end{Bmatrix} + z \begin{Bmatrix} \varepsilon_{xx}^{(1)} \\ \varepsilon_{yy}^{(1)} \\ \gamma_{xy}^{(1)} \end{Bmatrix}$$

$$= \begin{Bmatrix} \frac{\partial u_0}{\partial x} - \alpha_{xx} T_0 \\ \frac{\partial v_0}{\partial y} - \alpha_{yy} T_0 \\ \frac{\partial u_0}{\partial y} + \frac{\partial v_0}{\partial x} - \alpha_{xy} T_0 \end{Bmatrix} z \begin{Bmatrix} -\frac{\partial^2 w_0}{\partial x^2} - \alpha_{xx} T_1 \\ -\frac{\partial^2 w_0}{\partial y^2} - \alpha_{yy} T_1 \\ -2 * \frac{\partial^2 w_0}{\partial x \partial y} - \alpha_{xy} T_1 \end{Bmatrix}$$

eq. (9.a)



Eq. (2-21a) for linear varying of temperature i.e. [Reddy J.N.]

$$\Delta T = T_0(x, y, t) - zT_1(x, y, t) \tag{9.b}$$

In present work the varying of temperature supposed uniform, thus Eq. (2-21a) became

$$\begin{Bmatrix} \epsilon_{xx} \\ \epsilon_{yy} \\ \gamma_{xy} \end{Bmatrix} = \begin{Bmatrix} \frac{\partial u_0}{\partial x} - \alpha_{xx}\Delta T \\ \frac{\partial v_0}{\partial y} - \alpha_{yy}\Delta T \\ \frac{\partial u_0}{\partial y} + \frac{\partial v_0}{\partial x} - \alpha_{xy}\Delta T \end{Bmatrix} + z \begin{Bmatrix} -\frac{\partial^2 w_0}{\partial x^2} \\ -\frac{\partial^2 w_0}{\partial y^2} \\ -2 * \frac{\partial^2 w_0}{\partial x \partial y} \end{Bmatrix} \tag{9.c}$$

α_{xx} , α_{yy} and α_{xy} are thermal expansion coefficients defined

$$\alpha_{xx} = \alpha_{11}(\cos \theta)^2 + \alpha_{22}(\sin \theta)^2 \tag{10.a}$$

$$\alpha_{yy} = \alpha_{11}(\sin \theta)^2 + \alpha_{22}(\cos \theta)^2 \tag{10.b}$$

$$2\alpha_{xy} = 2(\alpha_{11} - \alpha_{22})\sin \theta \cos \theta \tag{10.c}$$

α_{11} and α_{22} Are longitudinal and transverse thermal expansions respectively. And θ is the lamination angle.

The change in temperature defined

$\Delta T = \text{applied temperature} - \text{reference temperature}$

Where reference temperature $T_{ref} = 25C^\circ$

The transformed stress-strain relations of an orthotropic lamina in a plane state of stress are; for \bar{Q}_{ij}

$$\begin{Bmatrix} \sigma_{xx} \\ \sigma_{yy} \\ \sigma_{xy} \end{Bmatrix} = \begin{bmatrix} \bar{Q}_{11} & \bar{Q}_{12} & \bar{Q}_{16} \\ \bar{Q}_{12} & \bar{Q}_{22} & \bar{Q}_{26} \\ \bar{Q}_{16} & \bar{Q}_{26} & \bar{Q}_{66} \end{bmatrix} \begin{Bmatrix} \epsilon_{xx} - \alpha_{xx}\Delta T \\ \epsilon_{yy} - \alpha_{yy}\Delta T \\ \gamma_{xy} - 2\alpha_{xy}\Delta T \end{Bmatrix} \tag{11}$$

$\{N^t\}$ and $\{M^t\}$ are thermal stress and bending results, respectively

$$\begin{Bmatrix} N_{xx}^t, M_{xx}^t \\ N_{yy}^t, M_{yy}^t \\ N_{xy}^t, M_{xy}^t \end{Bmatrix} = \sum_{k=1}^N \int_{-h/2}^{h/2} \begin{bmatrix} \bar{Q}_{11} & \bar{Q}_{12} & \bar{Q}_{16} \\ \bar{Q}_{12} & \bar{Q}_{22} & \bar{Q}_{26} \\ \bar{Q}_{16} & \bar{Q}_{26} & \bar{Q}_{66} \end{bmatrix} \begin{Bmatrix} \alpha_{xx} \\ \alpha_{yy} \\ 2\alpha_{xy} \end{Bmatrix} (1, z) \Delta T dz \tag{12}$$

The equation of motion is.

$$\begin{bmatrix} c_{11} & c_{12} & c_{13} \\ c_{12} & c_{22} & c_{23} \\ c_{13} & c_{23} & c_{33} \end{bmatrix} \begin{Bmatrix} u_0 \\ v_0 \\ w_0 \end{Bmatrix} + \begin{bmatrix} m_{11} & 0 & 0 \\ 0 & m_{22} & 0 \\ 0 & 0 & m_{33} \end{bmatrix} \begin{Bmatrix} \ddot{u}_0 \\ \ddot{v}_0 \\ \ddot{w}_0 \end{Bmatrix} = \begin{Bmatrix} 0 \\ 0 \\ q \end{Bmatrix} + \begin{Bmatrix} f_1^t \\ f_2^t \\ f_3^t \end{Bmatrix}$$

eq. (13)

Where

$$f_1^t = \frac{\partial N_{xx}^t}{\partial x} + \frac{\partial N_{xy}^t}{\partial y} \tag{14.a}$$

$$f_2^t = \frac{\partial N_{xy}^t}{\partial x} + \frac{\partial N_{yy}^t}{\partial y} \tag{14.b}$$

$$f_3^t = -\left(\frac{\partial^2 M_{xx}^t}{\partial x^2} + 2 \frac{\partial^2 M_{xy}^t}{\partial y \partial x} + \frac{\partial^2 M_{yy}^t}{\partial y^2} \right) \tag{14.c}$$

These equations of motion (13) can be expressed in terms of displacements ($\delta u_0, \delta v_0, \delta w_0$) by substituting the forces results from Eqs. (4,5,8,12,14 a-c) into Eq.(13) and get partial differential equations, then the analytical solution done by Navier method as derived in ref. [Reddy J.N.].

After applying Navier method, Newmark's direct integration method done.

2.2.2 Newmark's direct integration method

The term “direct” means that prior to the numerical integration; no transformation of the equations into a different form is carried out. Many numerical integration methods are available for the approximate solution of such equations of motion. All the numerical integration methods have two basic characteristics. First, they do not satisfy the differential equations at all-time t, but only at discrete time intervals, say Δt apart. Secondly, within each time interval Δt , a specific type of variation of the displacement, velocity and acceleration is assumed. ref. [Rao V. Dukkupati]

In the Newmark direct integration method, the first time derivative $\{\dot{U}\}$ and the solution $\{U\}$ are approximated at (n+1) time step (i.e. at time $t = t_{n+1} = (n+1)\Delta t$ by the following expression (ref[7]).

$$\{\dot{U}\}_{n+1} = \{\dot{U}\}_n + [(1-\bar{\alpha})\{\ddot{U}\}_n + \bar{\alpha}\{\ddot{U}\}_{n+1}] \Delta t \quad (15.a)$$

$$\{U\}_{n+1} = \{U\}_n + \{\dot{U}\}_n \Delta t + \left[\left(\frac{1}{2} - \bar{\beta} \right) \{\ddot{U}\}_n + \bar{\beta} \{\ddot{U}\}_{n+1} \right] (\Delta t)^2 \quad (15.b)$$

Where:

$\bar{\alpha}$ And $\bar{\beta}$: are parameters that control the accuracy and stability of the scheme, and the subscript n indicates that the solution evaluated at n^{th} time step (i.e. at time, $t = t_n$). The choice

$\bar{\alpha} = 0.5$ and $\bar{\beta} = 0.25$ is known to give an unconditionally stable Scheme (average acceleration method), [Rao V. Dukkipati].

Solving from Eq.(15.b) for $\{\ddot{U}\}_{n+1}$ in term of $\{U\}_{n+1}$, the acceleration at time t_{n+1} is obtained:

$$\{\ddot{U}\}_{n+1} = a_0 [\{U\}_{n+1} - \{U\}_n] - a_1 \{\dot{U}\}_n - a_2 \{\ddot{U}\}_n \quad (16)$$

The equilibrium Eq.(13) at time t_{n+1} is considered as:

$$[MA]\{\ddot{U}\}_{n+1} + [KS]\{U\}_{n+1} = \{R\}_{n+1} \quad (17)$$

Substituting from Eq.(16) into Eq.(17) and rearranging yields:

$$[\hat{M}]\{U\}_{n+1} = \{\hat{q}\}_{n+1} \quad (18)$$

Where:

$$[\hat{M}] = [KS] + a_0 [MA] \quad (19.a)$$

$$\{\hat{q}\}_{n+1} = \{R\}_{n+1} + [M] [a_0 \{U\}_n + a_1 \{\dot{U}\}_n + a_2 \{\ddot{U}\}_n] \quad \text{eq. (19.b)}$$

$$a_0 = \frac{1}{\bar{\beta}(\Delta t)^2}, \quad a_1 = \frac{1}{\bar{\beta}(\Delta t)}, \quad a_2 = \frac{1}{2\bar{\beta}} - 1$$

The first and second derivatives (\dot{U}, \ddot{U}) of $\{U\}$ at t_{n+1} can be computed from rearranging the expressions (15a-b):

$$\{\ddot{U}\}_{n+1} = a_0 [\{U\}_{n+1} - \{U\}_n] - a_1 \{\dot{U}\}_n - a_2 \{\ddot{U}\}_n \quad (20.a)$$

$$\{\dot{U}\}_{n+1} = a_3 (\{U\}_{n+1} - \{U\}_n) - a_4 \{\dot{U}\}_n - a_5 \{\ddot{U}\}_n \quad (20.b)$$

Where:

$$a_3 = \frac{\bar{\alpha}}{\bar{\beta}(\Delta t)}, \quad a_4 = \left(\frac{\bar{\alpha}}{\bar{\beta}} \right) - 1$$

$$a_5 = \frac{\Delta t}{2} \left(\frac{\alpha}{\beta} - 2 \right)$$

Once the displacements $\{U\}_{n+1}$ at time t_{n+1} are obtained by solving equation (18), the velocities $\{\dot{U}\}_{n+1}$ and accelerations $\{\ddot{U}\}_{n+1}$ are computed using Eqs.(20.a) and (20.b), respectively.

3. NUMERICAL ANALYSIS

3.1 Element selection and modeling

An element called shell281 as shown in Fig.1 is selected which is suitable for analyzing thin to moderately thick shell structures. The element has eight nodes with six degrees of freedom at each node: translations in the x, y, and z axes, and rotations about the x, y, and z axes. It may be used for layered applications for modeling composite shells. It includes the effects of transverse shear deformation. The accuracy in modeling composite shells is governed by the first order shear deformation theory. The shell section allows for layered shell definition, options are available for specifying the thickness, material, orientation through the thickness of the layers.

Finite element method has been employed to analyze natural frequency and dynamic response. The model was developed in ANSYS 14.0 using the 225 (15*15) quadrature elements. The global x coordinate is directed along the width of the plate, while the global y coordinate is directed along the length and the global z direction corresponds to the thickness direction and taken to be the outward normal of the plate surface. There are 15 elements in the axial direction and 15 along the width (i.e. 4416 DOF). Convergence study is the reasons for



choosing the particular mesh used in this study. A modal analysis was performed on the model to calculate the natural frequency of the structure. The transient analysis was performed on the modal to calculate the dynamic response (the program used Newmark method).

3.2 Verification Case Studies

In the present study, Series of preselected cases are modeled to verify the accuracy of the method of analysis. The results are compared to analytical solution (Levy) and numerical solution (Finite element method). see **Table 1** and **Table 2**. For dynamic response see **Fig.2** (no temperature effect) and **Fig.3** (with temperature effect).

From these results, it is obvious that the methods of solution gives better results for both analytical and numerical solution.

4. EXPERIMENTAL WORK

In the present work, Five- purposes were investigated. First, to outline the general steps to design and fabricate the rectangular test models from fiber (E-glass) and polyester resin to form laminate composite materials. Second, the manufactured models are then used to evaluate the mechanical properties (E_1, E_2, G_{12}) without temperature change of unidirectional composite material. Third, measure thermal conductivity for fiber-polyester composite plate and polyester, measure the temperature dependence of mechanical properties (E_1, E_2, G_{12}) and coefficient of thermal expansion (CTE) of the composite plate.

Fifth, the vibration test can be done to calculate the fundamental natural frequency of composite laminate plate for different boundary conditions cross ply laminate plate.

4.1 Tensile Test

Each laminate was oriented in longitudinal, transverse and 45° angle relative to designated 0° direction to determine the engineering parameters E_1, E_2, G_{12} . Tensile test specimen include standard geometry according to ASTM (D3039/D03039M); and the mechanical

properties for glass-polyester which obtained from tensile test as shown in **Table (3)**.

4.2 Thermo-Mechanical Analyzer

Thermo-mechanical Analysis (TMA) determines dimensional changes of solids and liquids materials as a function of temperature and/or time under a defined mechanical force.

Irrespective of the selected type of deformation (expansion, compression, penetration, tension or bending), every change of length in the sample is communicated to a highly sensitive inductive displacement transducer (LVDT) via a push rod and transformed into a digital signal. The push rod and corresponding sample holders of fused silica or aluminum oxide can be quickly and easily interchanged to optimize the system to the respective application. **Figs.4 and 5**.

The dimension of sample is (5*20*4) mm. the thermal properties which obtain from this test shown in **Table 4**.

4.3 Thermal conductivity test

Thermal conductivity coefficient of specimens was measured by using Lee's disk method principle. Very often composite materials results in anisotropic media and their thermal conductivity change along the axes because of the presences of reinforcing fibers embedded in the matrix.

The rule of mixture accurately predicts the thermal conductivity of fiber reinforced composite in both directions, [Louay S. Yousouf]:

When the fibers are arranged in the longitudinal direction, then:

$$K_1^c = K_f * v_f + K_m * v_m \quad (21.a)$$

When the fibers are arranged in the lateral direction:

$$K_2^c = \frac{K_f * K_m}{K_f * v_m + K_m * v_f} \quad (21.b)$$

Fig. (6) represents the test apparatus (Lee's disk apparatus) with tested composite specimen and some accessories to measure the temperature of both sides of the composite specimen in which direction x, y, z.

The heater is switch on with (V = 6 Volts and I = 0.25 Amp.) to heat the brass disks (2,3). And the temperatures were recorded every (5 minutes) until reach to the equilibrium

temperature of all disks. The fibers were arranged in the lateral direction and in the longitudinal direction.

Fig. 7 shows the sample used to measure the thermal conductivity using the Lee's Disk method is in the form of a disk whose thickness d_s is small relative to its radius (r) with ($d_1 = d_2 = d_3 = 12.25 \text{ mm}$). Using a thin sample means that the system will reach thermal equilibrium more quickly. When the fibers are arranged in the longitudinal direction ($r=21\text{mm}$) Coefficient of Thermal Conductivity $k_1 = 0.47068(W/M^\circ C)$

$$Ds=3.2 \text{ mm } T_A=31.2C^\circ T_B=34C^\circ T_C=34C^\circ$$

When the fibers are arranged in the transverse direction ($r=21\text{mm}$) Coefficient of Thermal Conductivity $k_2 = 0.33434(W/M^\circ C)$

$$Ds=3.75 \text{ mm } T_A=31 C^\circ T_B=35.5C^\circ T_C=35.5C^\circ$$

And the thermal conductivity can be calculated experimentally by using the following equation, [5]:

$$K * \left[\frac{T_2 - T_0}{d_s} \right] = e * \left[T_0 + \frac{2}{r} * \left(d_1 + \frac{1}{2} * d_s \right) * T_0 + \frac{1}{r} * d_s * T_2 \right] \quad (22.a)$$

And (e) can be evaluated from the following equation, [Louay S. Yousouf]:

$$I * V = \pi * r^2 * e * (T_0 + T_3) + 2 * \pi * r * e * \left[d_1 * T_0 + \frac{1}{2} * d_s * (T_0 + T_2) + d_2 * T_2 + d_3 * T_3 \right] \quad (22.b)$$

4.4 Vibration Test

The vibration test includes studying the first three frequencies for composite plate with different boundary condition four layers symmetric cross ply.

The dimensions of vibration plate samples used are, see **Fig. 8**.

$$a_t = a + 6cm \text{ (for supported)}$$

$$b_t = b + 6cm \text{ (for supported)}$$

For S-S-S-S and S-C-S-C, a and b equal to $20cm$, a_t and b_t equal to 26

But for S-F-S-F $b = 20cm$, $a = 26cm$, a_t and b_t equal to 26

The block diagram of the different instruments used for the measurements of natural

frequencies is shown in **Fig.9**. And the whole instruments that used in this test shown in **Fig. 10**.

The vibration structure rig is composed of the following parts

- (1) Frame Fixture: The composite laminate plate can be fixed according to the boundary conditions used a frame made from steel and supported (U-channel) made from steel to fix the composite plate.
- (2) The impact hammer: model (086C03) (PCB Piezotronics vibration division), stiff steel mass with many tips. The hammer consists of an integral quartz force sensor mounted on the striking end of hammer head. The sensing element functions to transfer impact force in to electrical signal for display and analysis. Impulse force test hammer is adapted for adapts FFT analysis of structure behavior testing. Impulse testing of the dynamic behavior of mechanical structure involves striking the test object with the force-instrumented hammer, and measuring the resultant motion with an accelerometer. When can be used the hammer is knocked the composite plate strongly or lightly that is effect on the value of amplitude; but the frequency still constant.
- (3) Accelerometer model (4371), accelerometer is a sensor that produces an electrical signal that is proportional to the acceleration of the vibrating component to which the accelerometer is attached. The accelerometer mounted to the plate by the screw which adhesive to the center of plate.
- (4) Amplifier, type 7749, the amplifier measures the response signal from accelerometer and gives output signal to the digital storage oscilloscope. It is a low noise charge amplifier for use with piezoelectric accelerometers and other piezoelectric transducers. It offers a wide range of signal conditioning that makes it ideal for use in accelerometers calibration set-ups and for general purpose vibration measurements.
- (5) Digital storage oscilloscope, modal GDS-810, has two input channels; this digital storage oscilloscope system can be driven with a computer. This device is used to display the response waves result, which extracted using accelerometer, for the



vibrated structures. Then analysis of response signal is read from digital storage oscilloscope to FFT function by using sig-view program to get the first three frequencies with different parameters studied.

5. RESULTS AND DISCUSSION

5.1 Experimental Results

The experimental results contain the first three frequencies in (HZ) for four layers symmetric cross ply for different boundary condition (SSCC, SSSS, SSFF) by using impact hammer the output signals appears on oscilloscope for each dynamic response which came from conditional amplifier which receives the dynamic response signal from accelerometer. Then analysis of response signal is read from digital storage oscilloscope to FFT function by using sig-view program to get the three frequencies of the plate. The experimental result gave good agreement when the analytical (CLPT with Levy method) and numerical (ANSYS) analysis compared with them maximum error is 8.7% for analytical by CLPT and 7.99% for numerical by ANSYS 14.0. The result shown in **Table 5**.

The maximum natural frequency occurs when the boundary condition is SSCC then the frequency decrease when the B.C's became SSSS with percentage 42.3% and then decreases when it became SSFF with percentage 76.9%.

5.2 Theoretical Results Contain (Analytical and Numerical (ANSYS))

5.2.1 Frequency result

In this section discussed the effect of different parameter on fundamental natural frequency such as boundary condition, aspect ratio, thickness ratio for symmetric cross ply composite laminate plate. This result found by analytical method using CLPT with Levy method and numerically using ANSYS 14.0 program.

5.2.1.1 Boundary condition

From the results listed in **Table 6** it can be observed that the boundary conditions always

effect on the fundamental natural frequency. It's worth mentioning the natural frequency in SCSC and SCSS for cross ply and SSSS are higher than other cases because of B.C'S. effect.

5.2.1.2 Aspect ratio

Fig.(11) for SSSS and SSCC cross ply shows that the natural frequency decrease when a/b increase with high percentage reaches to 68.7%. On the other hand the maximum natural frequency in case SSCC symmetric cross ply is at a/b=0.5. While the minimum is at SSSS symmetric cross ply for a/b=2.5.

5.2.1.3 Thickness ratio

It is shown from **Fig.12** for SSSS and SSCC four layers symmetric composite plate, the natural frequency decrease when thickness ratio increase. It can be observed that the natural frequency is decrease with high percentage when b/h varies from 10 to 20 reach to (70.15%). Then, this percentage gets smaller when b/h varies from 20 to 50 the maximum percentage reach to (53.96%). Also here the maximum natural frequency when SSCC boundary condition and a/h=10.

5.2.2 Dynamic response

The present study focused mainly on the dynamic response behavior of composite laminated plates subjected to mechanical and thermo-mechanical loads of finite duration uniform (step, sine and ramp) and sinusoidal (step, sine and ramp) on the top surface of the plate for three cases of temperature (without temperature effect, T=50°C and T=100°C). The step loading $q(x, y, t) = \bar{q}(x, y)$, ramp loading $q(x, y, t) = \bar{q}(x, y)t/t_1$ and sinusoid loading $q(x, y, t) = \bar{q}(x, y)\sin\pi t/t_1$. For uniform distributed load $\bar{q}(x, y) = \frac{16}{nm\pi^2}$ and for sinusoidal distributed $\bar{q}(x, y) = q_0$. The amplitude of force is $q_0 = 100N/mm^2$ and the time of load applied on plate is $t_1 = 0.05$ sec. The dynamic response of central deflection of composite plate discussed for different parameter such as load condition, aspect ratio,

temperature value for symmetric cross ply for simply supported composite plate analytically by CLPT with Newmark direct integration method and numerical result by ANSYS.

5.2.2.1 Effect of load condition

Fig.13 and **Fig.14** represent the variation of central transverse deflection with time (dynamic response) for four layer symmetric cross-ply simply supported laminated plates under sinusoidal

$(P(x,y) = q_0 \sin(\pi x/a) \sin(\pi y/b))$ and uniform $(P(x,y) = q_0)$ variation loading, (step $q(x,y,t) = P(x,y)$, ramp loading $q(x,y,t) = P(x,y) t/t_1$ and sinusoid loading $q(x,y,t) = P(x,y) \sin \pi t/t_1$) for $q_0 = 100 \text{ N/m}^2$, $t_1 = 0.05 \text{ sec}$) without any temperature change solved by analytically by CLPT with Newmark direct integration method and (F.E.M) by ANSYS program. The deflection due to step loading higher in magnitude than the other loads with percentage reach to 91.96%, 97.4% from sine and ramp load, respectively, because the step load subjected suddenly with constant value with the time. Very good verification between CLPT with Newmark and FEM by ANSYS maximum error is 12.9%. Maximum response for step load always occurs in the time of applying load (i.e. in the time less than t_1 after that the response became in negative sign and positive sign alternatively. for ramp load, the response increasing linearly with time until it reached to t_1 at this point the maximum response occurs, then the response became in negative sign and positive sign alternatively. For sine load the response behavior have the sine shape and the maximum response at $t_1/2$.

5.2.2.2 Effect of temperature change with varies load condition

Fig 15 to **Fig. 20** show the numerical result by ANSYS for dynamic response of central deflection of symmetric cross ply simply supported composite plate under different kind of load and different condition of temperature effect i.e. (T=25°C, T=50°C, T=100°C). The deflection increase with maximum percentage

reaches to (58.47%) when temperature became 50°C and when the temperature reach to 100°C the response increase with higher percentage reaches to (200%) with respect to response without change in temperature.

5.2.2.3 Effect of aspect ratio

Fig. 21 shows the effect of the aspect ratio (a/b) on the deflection of the simply supported symmetric cross-ply laminated plates (b=200 mm) subjected to step sinusoidal loading without temperature change solved by F.E.M. From the results, increasing (a/b) ratio increasing the deflection of laminated plates. The increase in deflections is 92.4%, 92.8% for increasing aspect ratio (0.5 to 1.5) and (1.5 to 2) respectively.

6. CONCLUSION

This study considers the vibration analysis of symmetric cross-ply composite laminate plate with various B.C's. From the present study, the following conclusions can be made:

- 1- The Young and shear modulus decrease when temperature increases with high percentages reach to 96.3% when temperature changes from (20 °C to 100°C) for longitudinal young modulus, for transverse young modulus is 96.53% and for shear modulus is 91.1%. The longitudinal and transverse coefficient of thermal expansion also decrease when temperature increase with percentage 80% and 73.7% respectively for the same temperature.
- 2- The boundary conditions effect on the natural frequency, the maximum frequency occurs when there were clamped in boundary condition of plate. The percentage of increasing the natural frequency when the B.C's change from SSSS to SSCC 45.4% and the percentage of increasing natural frequency when changing B.C's from SSFF to SSCC is 75.5% for symmetric cross ply.
- 3- The fundamental natural frequency of composite laminated plate is decreasing when a/b increase with high percentage reaches to 68.7%.
- 4- The natural frequency decrease when thickness ratio increases. It can be observed that the natural frequency is decrease with high



percentage when b/h varies from 10 to 20 reach to (70.15%). Then, this percentage gets smaller when b/h varies from 20 to 50 the maximum percentage reach to (53.96%).

5- The response due to step loading higher in magnitude than the other loads with percentage reach to 91.96%, 97.4% from sine and ramp load, respectively, because the step load subjected suddenly with constant value with the time.

6- The response increase with maximum percentage reaches to (58.47%) when temperature became 50°C and when the temperature reach to 100°C the response increase with higher percentage reaches to (200%) with respect to response without change in temperature. The reason behind that is there are two loads (mechanical and thermal) each of load cause the deflections (thermal and mechanical deflections) summation is the deflection of plate under thermo-mechanical loading. When the temperature increase the deflection increase with high percentage.

7- Increasing of aspect ratio (a/b) increasing the response of laminated plates. The increase in deflections reach to 92.4%, 92.8% for increasing aspect ratio (0.5 to 1.5) and (1.5 to 2) respectively for simply supported symmetric cross-ply laminated plates subjected to step sinusoidal loading without temperature change .

7. REFERENCES

- Chornng-Fuh Liu and Chih-Hsing Huang, 1996, "Free Vibration of Composite Laminated Plates Subjected to Temperature Changes" Computers & Structures, Vol. 60, pp. 95-10.
- Dobyns A. L.; "Analysis of Simply Supported Orthotropic Plates Subjected to Static and Dynamic Loads", 1981, ALAA J., Vol. 19, No .3, p.p. 642-650.
- Hui-Shen Shen, J. J. Zheng and X. L. Huang, 2003, "Dynamic Response of Shear Deformable Laminated Plates Under Thermomechanical Loading and Resting on Elastic Foundations", Composite Structures, Vol. 60, pp. 57-66.
- Kullasup Phongsrisuk, Prasong Ingsuwan, Wetchayan Rangsi and Wiwat Klongpanich, "Free vibration analysis of symmetrically laminated composite rectangular plates using extended Kantorovich method" 2010, Maejo International Journal of Science and Technology ISSN 1905-7873, 4(03), 512-532.
- Louay S. Yousouf, "Time Prediction of Dynamic Behavior of Glass Fiber Reinforced Polyester Composites Subjected to Fluctuating Varied Temperatures" 2007, AL-Khwarizimi engineering Journal, vol5, no3, pp28-37(2009).
- Metin Aydogdu, Taner Timarci, "Free Vibration of Antisymmetric Angle-Ply Laminated Thin Square Composite Plates" Turkish J. Eng. Env. Sci 31,243-249
- Rao V. Dukkipati "Matlab an Introduction with Applications" New age international publishers. ISBN(13):978-81-224-2920-6 (2010).
- Reddy J. N.; "On the Solution to Forced Motions of Rectangular Composite Plates" 1982, J. Applied Mechanics, Vol. 49, p.p. 403-408.
- Reddy J.N. "Mechanics of Laminated Composite Plates and Shells: Theory and Analysis ". 2ed; CRC Press 2004.
- Suresh Kumar J., Dharma Raju T. and Viaya Kumar Reddy K., "Vibration Analysis of Composite Laminated Plates Using Higher Order Shear Deformation Theory with Zig-Zag Function" 2011, Indian journal of science and technology vol.4 ,no.8,ISSN:0974-6846.
- "Theory, Analysis, and Element Manuals" ANSYS 13 Program.

8. NOMENCLATURE

Symbol	Description	Unit
a, b	Dimension of plate in x and y coordinate	m
A_{ij}, B_{ij}, D_{ij}	Extensional stiffness, the coupling stiffness, and the bending stiffness	-
d_1, d_2, d_3	Thicknesses Of The Brass Disks	m
D_c	Thickness Of The Composite Specimen	m
E_1, E_2, E_3	Elastic modulus of composite material	GPa
G_{12}, G_{23}, G_{13}	Shear modulus of composite material	GPa
h	Thickness	m
I	Ampere	Amp.
i	Imaginary Root = $\sqrt{-1}$	-
I_0, I_1, I_2	Mass moment of inertia	kg.m ²
k_1, k_2	Coefficient of Thermal Conductivity of composite material	(W/m ² C)
k_f, k_m	Coefficient of Thermal Conductivity of fiber and matrix respectively	(W/m ² C)
[MA]	Mass matrix	kg
M_{xx}, M_{yy}, M_{xy}	Moment resultant per unit length	N.m/m
N	Total number of plate layers	-
N_{xx}, N_{yy}, N_{xy}	The resultant of in-plane force per unit length	N/m
$\bar{N}_{xx}, \bar{N}_{yy}, \bar{N}_{xy}$	Applied edge force	N/m
q(x,y,t)	Dynamic force subjected on a system	N/m ²
$\bar{Q}_{ij}^{(k)}$	Transformed lamina stiffness	N/m
R	Vector of externally applied loads	N
r	Disk spacemen Radius	m
t	Time	min or s
Δt	Time Interval	min or s

t_1	The end time of load	sec
T	Temperature	C ⁰
ΔT	Temperature increment	C ⁰
T_A, T_B, T_C	Temperature across the sample sides	C ⁰
T_{ref}	Reference temperature	C ⁰
U, \dot{U}, \ddot{U}	Displacement , velocity and acceleration vectors	m, m/s, m/ s ²
u_x, v_x, w_x	Displacement components along (x,y,z) directions respectively	m
$U_{max}, V_{max}, W_{max}$	Aamplitudes of (u_x, v_x, w_x) respectively	-
V	Voltage	Volt
V_f	Fiber volume fraction	-
V_m	Matrix volume fraction	-
w	Natural frequency	Hz
\bar{w}	Nondimensional frequency	Hz
x, y, z	Cartesian coordinate system	m
z	Distance from neutral axis	m
θ	Fiber orientation angle	Degree
α_1, α_2	Coefficient of thermal expansion of composite material	(1/C ⁻²) or (1/K ⁻²)
ρ	Density	(kg/m3)
$\epsilon_{xx}, \epsilon_{yy}, \epsilon_{xy}$	Strain components	m/m
$\sigma_{xx}, \sigma_{yy}, \sigma_{xy}$	Stress components	GPa

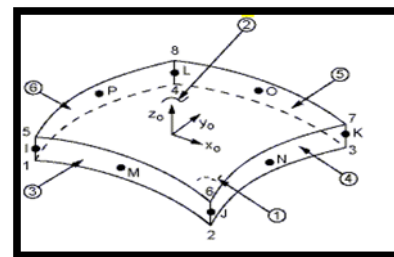


Figure . 1, Shell281 Geometry [ANSYS 13 Program]

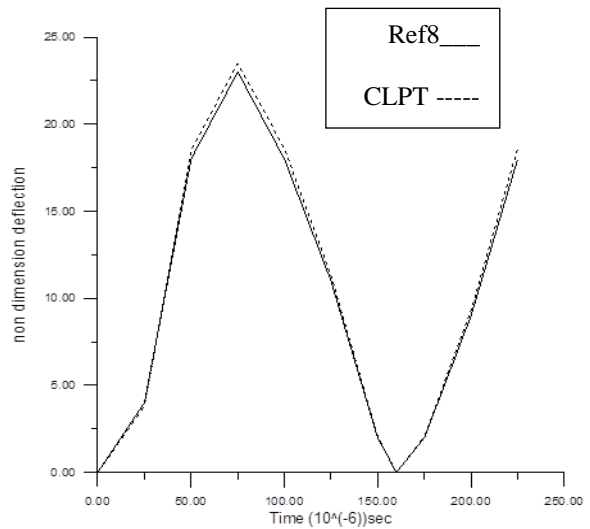


Table 1. Dimensionless natural frequency $\bar{\omega} = \omega a^2 \sqrt{\frac{\rho}{E_2 h^2}}$ of simply support symmetric cross ply laminates

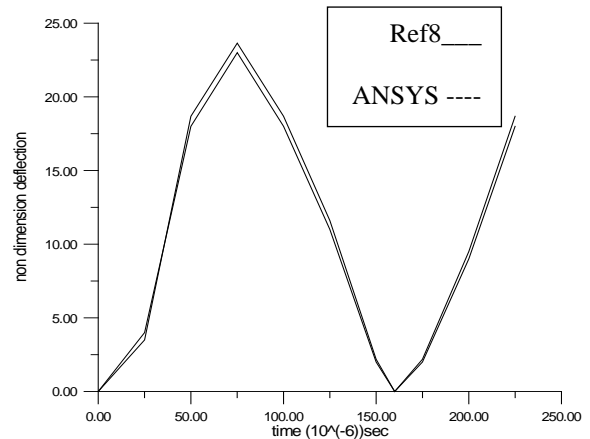
a/h	[3] [HOSDT]	Present [ANSYS14.0] (Error %)	$E1/E2=40$ $G12=G13=0.6E2$ $G23=0.5 E2$ $\nu12=0.25$ $a = b$ $h=1$ $\rho=1kgm^{-3}$ orientation 0/90/0
5	10.263	10.12888 (1.3%)	
10	14.702	14.67395 (0.19%)	
20	17.483	17.45982 (0.13%)	
25	17.95	17.91815 (0.178%)	
50	18.641	18.62768 (0.0715%)	
100	18.828	18.79517 (0.174%)	

Table 2. Dimensionless natural frequency $\bar{\omega} = \frac{\omega b^2}{h} \sqrt{\frac{\rho}{E_2}}$ of anti-symmetric cross ply laminates

B.C'S	b/a	[9] CLPT(levy method)	present CLPT(levy method) (Error %)	$E1/E2=40$ $G12=G13=0.6 E2$ $G23=0.5 E2$ $\nu12=0.25$ $a/h=10$ $h=1m$ $1kgm^{-3}=\rho$ orientation 0/90
S-C-S-C	1	18.543	19.365(4.4 %)	
S-C-S-C	2	64.832	63.875 (1.48 %)	
S-C-S-C	3	137.71	140.728 (2.1 %)	
S-S-S-S	1	11.154	11.292 (1.24 %)	
S-S-S-S	2	30.468	31.749 (4 %)	
S-S-S-S	3	63.325	65.36 (3.11%)	
S-F-S-F	1	7.267	7.54 (3.6 %)	
S-F-S-F	2	7.267	7.32 (0.73 %)	
S-F-S-F	3	7.267	7.742093 (6.5 %)	

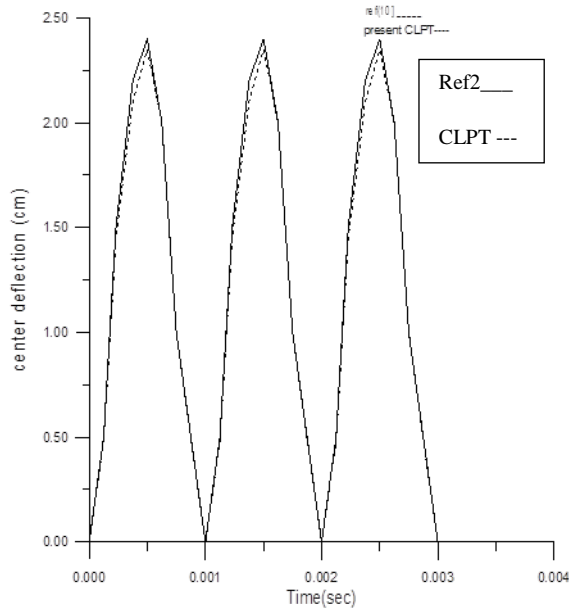


a1

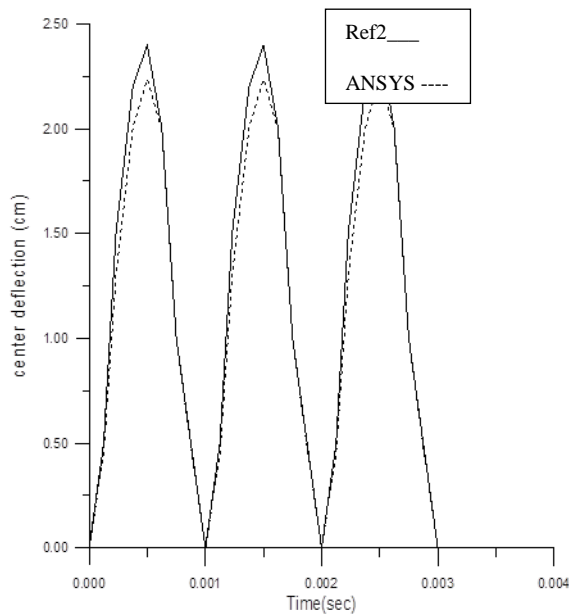


a2

Figure 2. Comparison of the present solution with the numerical solution of Reddy [8] of two-layer cross-ply (0/90) square plate under suddenly applied sinusoidal loading (a1-analytical with CLPT, a2-numerically with ANSYS).



A1



A2

Figure 3. Comparison of present study with Hui-Shen Shen et al [3] for laminated square plate under thermal loading condition at ($\Delta T = 200 C^0$).

Table 3. Experimental unidirectional mechanical properties of fiber glass-Polyester with fiber volume fraction 0.3 (Density $\rho=1496.286 \text{ kg/m}^3$).

property	Fiber-polyester composite plate
Young modulus E_1 (Mpa)	22049.793
Young modulus E_2 (Mpa)	4163.89
Shear Modulus G_{12} (Mpa)= G_{13}	1428.753
Shear Modulus G_{23} (Mpa)= G_{13}	1428.753

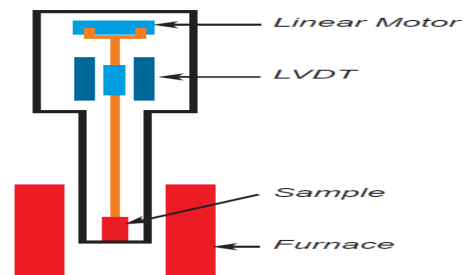


Figure 4. operating principle of TMA.



Figure 5. TMA PT1000 device.

Table4. Experimental value of mechanical and thermal properties of fiber –polyester composite plate for fiber volume fraction= 0.3 changed with temperature.

T C°	E ₁ Mpa	E ₂ Mpa	G ₁₂ =G ₁₃ = G ₂₃ Mpa	α ₁ E-6/K	α ₂ E-6/K
20	24627.0	5588.04	1551.77	14.57	47.81
30	23343.30	4123.11	1618.65	9.03	31.7
40	21775.40	1550.22	2505.75	7.20	29.36
50	15219.80	1515.37	623.423	4.79	25.79
60	6475.41	566.8	114.2336	3.20	21.38
70	2990.82	458.59	113.535	3.18	15.60
80	2555.71	289.27	130.48	3.22	15.59
90	1471.90	210.49	158.83	3.08	15.19
100	903.90	193.84	138.48	2.91	12.58
110	741.31	191.75	131.74	2.75	11.57
120	674.40	187.53	125.23	2.57	10.47
130	644.70	186.51	122.56	2.48	9.34
140	629.01	185.19	117.59	2.45	7.67
150	612.02	182.66	107.81	2.44	5.28
160	597.61	181.88	100.28	2.44	4.19
170	592.41	173.50	95.414	2.44	3.90
180	592.22	164.55	95.04	2.45	3.88
190	591.02	163.91	85.71	2.46	3.66
200	590.57	153.3	83.64	2.47	3

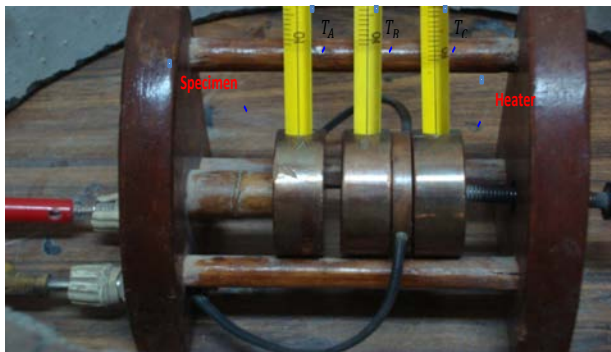
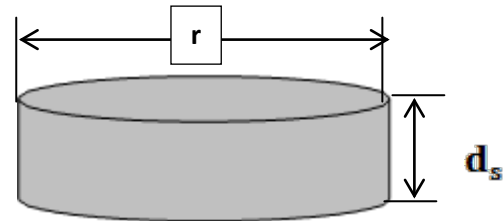


Figure 6. Lee's disk apparatus.



a- Thermal conductivity specimen



b- Dimension of thermal conductivity specimen

Figure 7. Thermal conductivity specimen dimension.

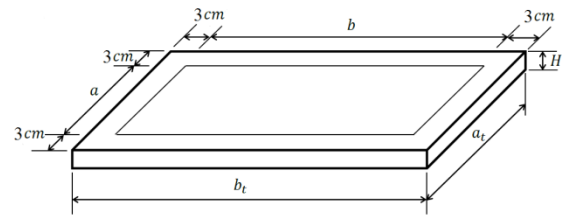


Figure 8. Dimensions of plate that used in vibration test.

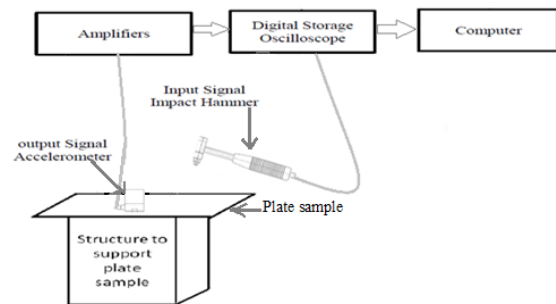


Figure9. Block diagram of vibration structure rig.

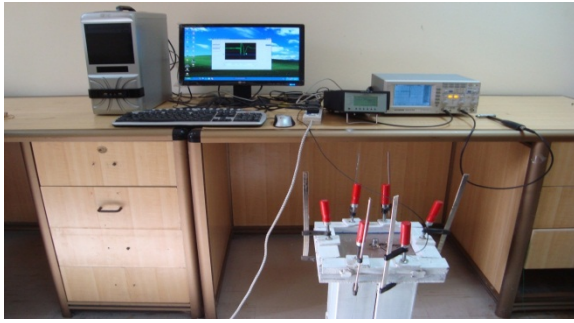


Figure 10. Rig and Vibration Test Machine of Composite Plate Structure.

Table 5. First three frequencies in (HZ) for four layers symmetric cross ply with different B.C's

B.C's	CLPT (Levy) (Error %)	Finite element ANSYS (Error %)	Experimental
SSCC	410.15(2.2%)	401.04(0.10%)	401.461
	581.23(3.5%)	576.84(4.2%)	602.192
	963.8(2.5%)	981.21(0.71%)	988.21156
SSSS	223.96(3.2%)	217.533(6%)	231.479
	458.5(1%)	460.712(0.6%)	463.2736
	724.2(4.3%)	696.239(7.99%)	756.733
SSFF	100.66(8.7%)	94.037(1.5%)	92.644
	120.8(2.3%)	119.657(3.2%)	123.65
	301.97(2.9%)	288.314(1.7%)	293.36

Table 6. Effect of boundary condition on natural frequency in (HZ) (0/90/90/0).

Boundary condition	Analytical Levy	F.E.M ANSYS (Error%)
S-C-S-C	410.15	401.04 (2.2%)
S-S-S-S	223.96	217.533 (2.9%)
S-F-S-F	100.66	93.99 (6.6%)
S-F-S-C	120.77	124.66 (3%)
S-C-S-S	304.5	296.75 (2.5%)
S-F-S-S	105.68	105.7 (0.02%)

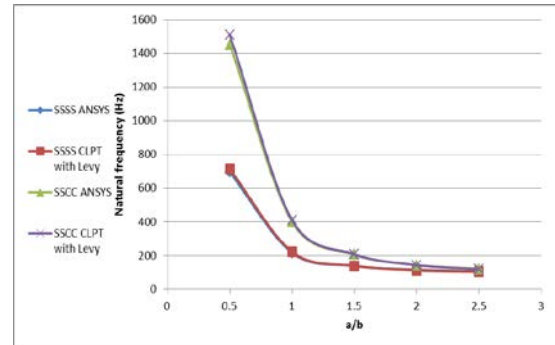


Figure 11. Effect of aspect ratio for symmetric cross plies on natural frequency.

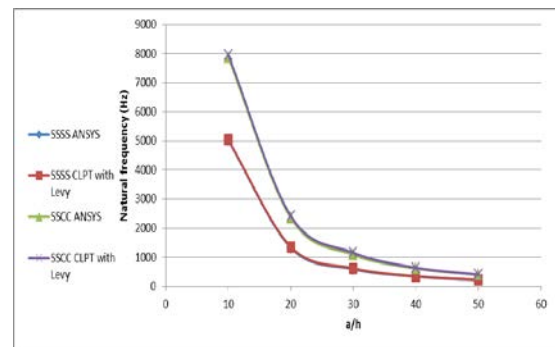


Figure 12. Effect of thickness ratio for symmetric cross plies on natural frequency.

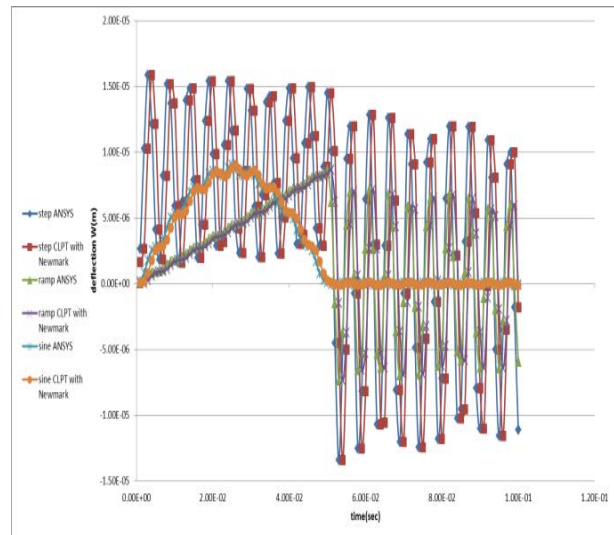


Figure 13. Central deflection of four layers symmetric cross-ply laminated plates for variant sinusoidal dynamic load without temperature change.

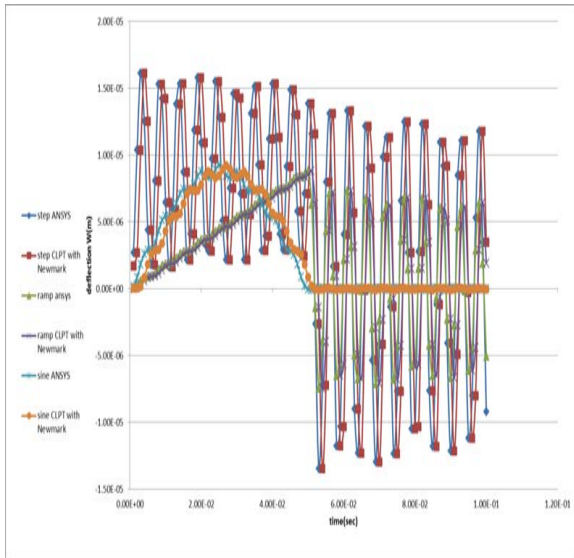


Figure 14. Central deflection of four layers symmetric cross-ply laminated plates for variant uniform dynamic load without temperature change.

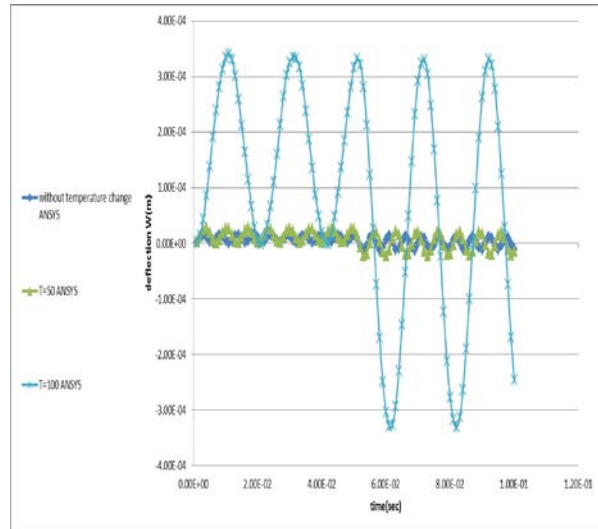


Figure 16. Central deflection of four layers symmetric cross-ply laminated plates for step sinusoidal dynamic load with temperature change.

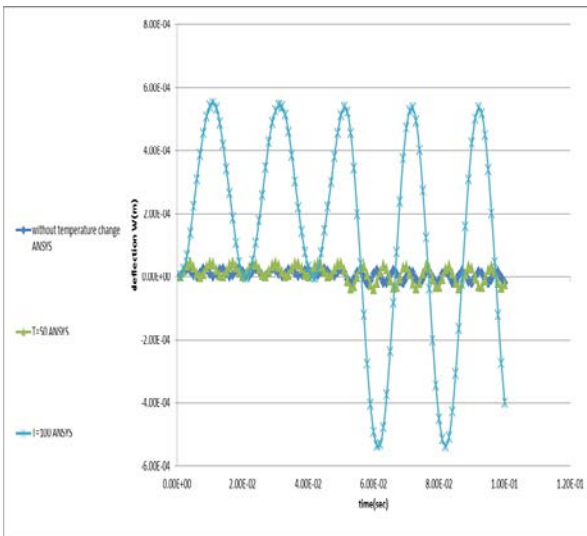


Figure 15. Central deflection of four layers symmetric cross-ply laminated plates for step uniform dynamic load with temperature change.

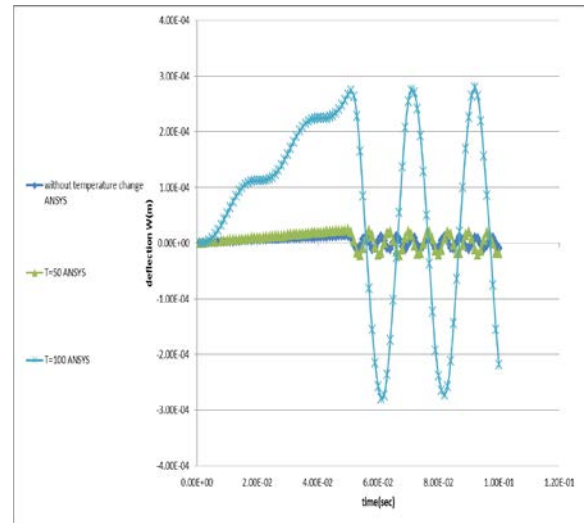


Figure 17. Central deflection of four layers symmetric cross-ply laminated plates for ramp uniform dynamic load with temperature change.

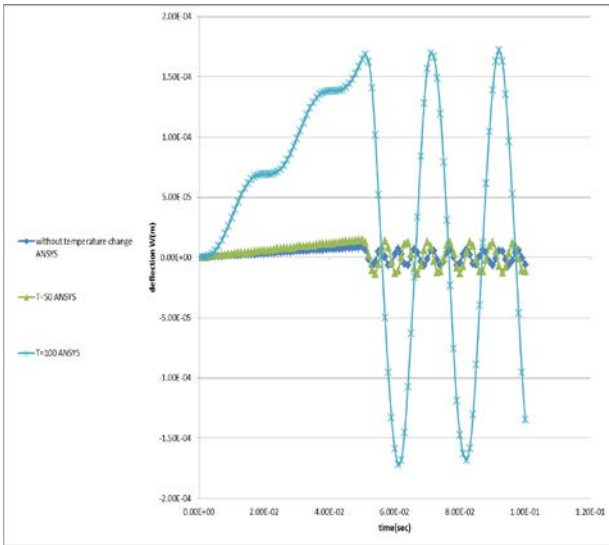


Figure 18. Central deflection of four layers symmetric cross-ply laminated plates for ramp sinusoidal dynamic load with temperature change.

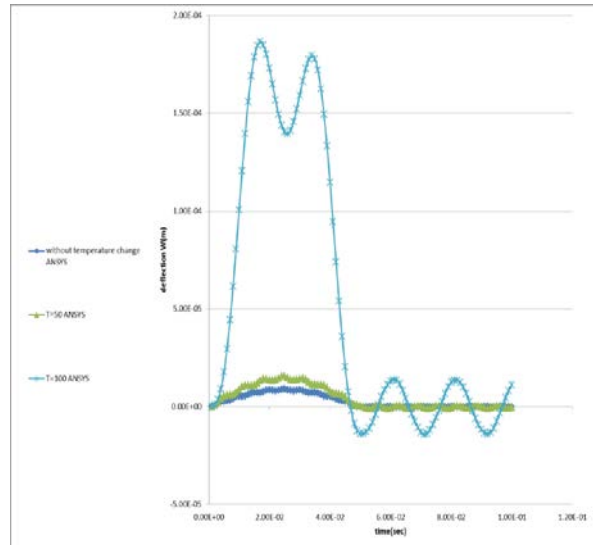


Figure 20. Central deflection of four layers symmetric cross-ply laminated plates for sine sinusoidal dynamic load with temperature change.

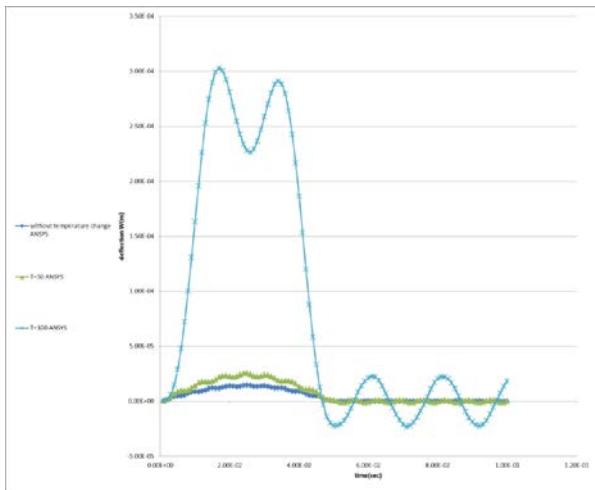


Figure 19. Central deflection of four layers symmetric cross-ply laminated plates for sine uniform dynamic load with temperature change.

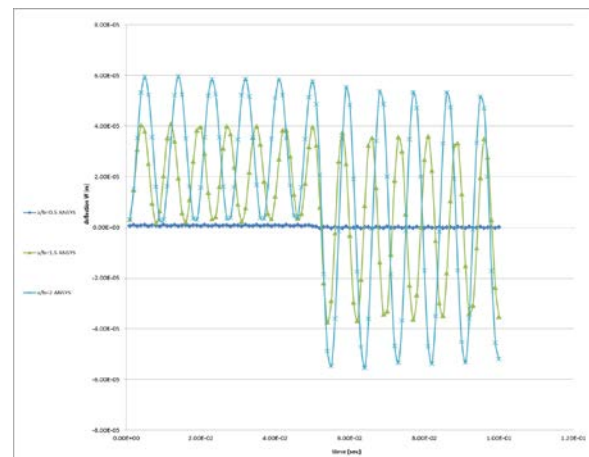


Figure 21. Effect of aspect ratio on central deflection of four layers symmetric cross -ply laminated plates for step sinusoidal dynamic load without temperature change.



Number 2

Volume 20 February 2014

Journal of Engineering